or pellets containing silica. The strength of pellets or sinters, on the other hand, is likely to improve as a result of fayalite formation. This is because fayalite, as shown here, has a tendency to cover the surfaces of particles whereby it establishes crystalline bonds between nearby grains.

CONCLUDING REMARKS

It has been shown here that fayalite forms in the reduction of Carol Lake material by $CO+CO_2$ mixtures (in the magnetite stability range) as a side reaction between the product magnetite and impurity silica. The reaction becomes important at temperatures of 1000°C and above.

During reduction at 1100°C fayalite has been found to form preferentially on the surfaces of magnetite particles. Theoretical considerations indicate that this mode of growth may be a result of oxygen removal from magnetite surfaces which is required to take place simultaneously with the formation of fayalite.

The formation of fayalite as a covering layer on magnetite surfaces results in the sites of silica particles in the original pellet being left vacant. This is confirmed by an increase in porosity from 0·29 to 0·42 at 1100°C and by the appearance of very large pores.

Theoretical considerations and information from previous work indicate that fayalite is an undesirable constituent since it is detrimental to reducibility. The effect of fayalite formation can be minimized by keeping magnetite formation temperatures below 1000°C and preventing prolonged exposure of magnetite to the reducing gas atmosphere. Temperatures of 1100°C and above should be avoided because of the formation of liquid phases.

ACKNOWLEDGMENTS

The author would like to thank Prof. A. V. Bradshaw for the supervision of this work and Dr J. Williamson for his help in the identification of fayalite. This work was carried out in the tenure of a post-graduate studentship from the University of London.

REFERENCES

1. B. G. BALDWIN: *J. Iron Steel Inst.*, 1954, **177**, 312–316.
2. A. ÜNAL and A. V. BRADSHAW: *Metall. Trans.*, 1983, **14B**, 743–752.
3. A. ÜNAL: PhD thesis, University of London, 1975.
4. L. S. DARKEN and R. W. GURRY: *J. Am. Chem. Soc.*, 1945, **67**, 1398–1412.
5. O. KUBASCHEWSKI and C. B. ALCOCK: 'Metallurgical thermochemistry', 5 edn, 342–345; 1979, Oxford, Pergamon Press.
6. R. SCHENCK, H. FRANZ, and A. LAYMAN: *Z. Anorg. Allg. Chem.*, 1932, **206**, 129–151.
7. V. CIRILLI: *Gaz. Chim. Ital.*, 1946, **76**, 331–338.
8. K. SCHWERDTFEGER and A. MUAN: *Trans. AIME*, 1966, **236**, 201–211.
9. 'JANAF thermochemical tables', PB 168 370–1 and PB 168 370–2; 1967, Washington, DC, US Dept of Commerce.
10. B. G. LEBEDEV and V. A. LEVITSKY: *Zh. Fiz. Khim.*, 1962, **36**, 630–632.
11. A. MUAN: *Trans. AIME*, 1955, **203**, 965–976.
12. L. S. DARKEN: *J. Am. Chem. Soc.*, 1948, **70**, 2046–2053.
13. M. HILLERT: *Metall. Trans.*, 1985, **16A**, 137–139.
14. A. V. BRADSHAW and A. G. MATYAS: *Metall. Trans.*, 1976, **7B**, 81–87.
15. H. SCHMALZRIED: 'Solid state reactions', 94–97; 1974, New York, Academic Press.
16. E. M. LEVIN, C. R. ROBBINS, and H. F. McMURDIE (eds.): 'Phase diagrams for ceramists', 241; 1964, Columbus, Ohio, American Ceramic Society.

Mechanical properties of formcoke

T. E. Easler, R. C. Bradt, and P. L. Walker, Jr

The mechanical properties of two formcokes being considered for use as alternative blast-furnace fuels were determined as a function of bulk density. The elastic moduli, fracture toughness, and fracture surface energies were measured with methods conventionally used for other brittle materials. Each of these properties was observed to increase with increasing bulk density. IS/590

 Manuscript received 22 August 1984; in final form 23 January 1985. At the time the work was carried out the authors were in the Department of Materials Science and Engineering, Pennsylvania State University, University Park, Pa, USA. Dr Easler is now with the Materials Science and Technology Division, Argonne National Laboratory, Argonne, Ill. and Dr Bradt is now in the Department of Materials Science and Engineering, University of Washington, Seattle, Wash.

INTRODUCTION

Formcoke has been given serious consideration as an alternative fuel for use in blast furnaces and other metallurgical applications. The prospect of decreasing availability and increasing expense of good coking coals has especially promoted this interest. Unlike conventional metallurgical cokes which are prepared from a relatively narrow range of bituminous coking coals, formcoke may be prepared from more widely available non-coking coals.[1,2] Several different processing methods may be used to obtain the desired size and shape pieces of formcoke. Some include separating the precursor coal into its volatile and non-volatile components, or pitch and char, respectively. The pitch and char are then further processed, recombined, and moulded into briquettes. The formcoke is then carbonized to obtain the final product. These processes are discussed further below.

Historically, the formcoke concept originated several decades ago. Early attempts at maintaining briquetting operations were generally unsuccessful because of processing and economic problems. Contemporary formcoke plants have evolved to the point where three general types of processing are recognized. These include (i) direct briquetting of crushed raw coal followed by carbonization; (ii) high-temperature carbonization of the coal, followed by crushing, mixing with pitch, briquetting, and carbonization; and (iii) low-temperature separation of tar and char, char calcining, recombination of char and tar, briquetting, and carbonization. The third processing method was used in this study.[3,4] Although relatively few blast-furnace trials have been completed using formcoke, most documented results have yielded promising indications.

The requirements and characteristics of coke that are necessary to blast-furnace operation must be taken into consideration in formcoke production.[5] Size and shape are important in determining coke/ore contacts and the amount of void space in the blast furnace, which is necessary to allow the flow of gases and liquids through the burden. The strength and reactivity of the coke are critical parameters. In particular, the mechanical properties of formcoke are a major concern because of the load-bearing requirements in the blast furnace. In this paper some of the mechanical properties of two slightly different formcokes are discussed. It is shown that conventional mechanical-properties tests for brittle materials can be successfully applied to formcoke.

EXPERIMENTAL PROCEDURE

MATERIALS

The raw coal used in preparation of the formcokes for this study was Illinois no. 6 from the Sesser mine. Proximate and ultimate analyses are given in Table 1. The analyses indicate that the coal rank is high-volatile C bituminous. Several steps were involved in the initial processing.* The dried coal was crushed to 100% less than 3·2 mm in size. These particulates were then pre-oxidized at 180°C to remove any caking characteristics they may have retained. The next step was heat treatment at 500°C, during which two different chars were produced by treatment in either an air–N_2 or O_2–steam environment. It is during this stage that the volatile (tar) component is removed from the non-volatile (char) component of the coal. The chars were then calcined at 815°C in environments similar to those used in the carbonizer. Calcination causes shrinkage of the char particulates as they are further carbonized. Proximate and ultimate analyses of the chars are given in Table 1. The tar was also processed by introducing air at 100°C to produce a pitch having the chemical analysis given in Table 2. The final stages of preparation resulted in two different char–

*Initial processing completed at Inland Steel Co., East Chicago, Ind.

Table 1 Analyses of coal and chars*

	Proximate analysis (dry basis), wt-%				Ultimate analysis, wt-%†															
	Volatile matter	Fixed C	Ash	S	Moisture ar	Moisture db	C ar	C db	H ar	H db	N ar	N db	Cl ar	Cl db	S ar	S db	O ar	O db	Ash ar	Ash db
Illinois no. 6 coal	35·9	58·2	5·8	0·7	5·1	...	73·0	77·0	4·8	5·1	0·9	1·0	0·4	0·4	0·7	0·7	9·1	9·6	5·9	6·2
Air–N_2 char	3·4	85·7	10·9	‡	6·7	...	79·0	84·7	1·1	1·2	1·1	1·2	...	...	0·6	0·7	3·2	3·4	8·3	8·9
O_2–steam char	3·5	86·8	9·7	‡	1·8	...	84·2	85·8	1·1	1·1	1·5	1·6	...	...	0·6	0·6	2·9	2·9	7·9	8·0

*Analyses performed at Inland Steel Pilot Plant, East Chicago, Ind.
† ar as received; db dry basis.
‡Not measured.

Table 2 Chemical analysis of pitch, wt-%*

C	O	H	N	Ash
80·4	9·8	6·8	1·5	1·6

*Analysis performed at Inland Steel Pilot Plant, East Chicago, Ind.

pitch systems. The two chars were then mixed with pitch at room temperature in a ratio of 40 parts by weight of pitch per hundred parts total.* The mixture was heated to 85°C and moulded into rectangular bars $127 \times 25 \times 13$ mm in size. Rectangular bars were moulded specifically for this study to facilitate the mechanical-properties measurements, although formcoke is conventionally moulded in the form of pillow-shaped briquettes. The bars were subsequently carbonized at 870°C to obtain the final product. Those bars prepared with the air–N_2 calcined char are referred to as the air–N_2 formcoke while the second type are referred to as the O_2–steam formcoke.

PROPERTIES

Before characterizing various physical properties and mechanical properties of the formcoke specimens, because of their highly hygroscopic nature they were dried at 120°C. Some of the physical properties of the two formcokes are given in Table 3.

Several mechanical properties were determined. The tests selected for this study are those conventionally used for brittle materials. Although tumble tests are usually used to characterize the mechanical breakdown of coke, it is difficult to quantify the test results. The tests described below yield results which can be described in terms of accepted international units; they were found to be satisfactory in characterizing the brittle formcoke materials.

The Young's elastic modulus E, the elastic shear modulus G, and Poisson's ratio ν were measured using the dynamic mechanical resonance technique which relates the resonant frequency of the specimen to the elastic moduli.[6,7] Fracture toughness K_{Ic} was determined by fracturing straight-notched beams in three-point bend, generally known as the notched-beam test.[8] Two different fracture surface energies were measured.[9,10] The fracture initiation surface energy, or γ_{NBT}, is the amount of energy which must be stored in the specimen in order to initiate fracture; this measurement was also made via the notched-beam test. The quasi-static fracture propagation surface energy, or γ_{WOF}, was determined via the work-of-fracture technique, in which a chevron-notched beam is fractured slowly in a stable fashion. The total amount of energy to propagate a crack completely through the specimen is taken as γ_{WOF}. Diagrams of the γ_{NBT} and γ_{WOF} test geometries are shown in Fig. 1. All of the mechanical-properties measurements were carried out at room temperature. Since a range of bulk densities was observed for each of the two formcokes, with some of the O_2–steam formcoke specimens falling at slightly lower densities than the air–N_2 formcoke, the mechanical properties of each were related to their bulk densities. Bulk densities were calculated from the specimen mass and dimensions.

RESULTS AND DISCUSSION

ELASTIC MODULI

As indicated in Table 3, the bulk density for the O_2–steam formcoke specimens ranged from 0·70 to 0·94 Mg m^{-3}, while that for the air–N_2 formcoke varied from 0·78 to 0·99 Mg m^{-3}. The elastic moduli were measured for specimens taken over the entire range of densities. The

*Final processing completed at Airco Speer Carbon and Graphite, Niagara Falls, NY.

Table 3 Physical properties and characteristics of formcokes

Property*	O_2–steam formcoke	Air–N_2 formcoke
Bulk density, Mg m^{-3}		
Range	0·70–0·94	0·78–0·99
Average	0·83	0·88
X-ray density, Mg m^{-3}	2·07	2·07
Surface area, m^2 g^{-1} (CO_2, 298 K)	475	485
Porosity (open to H_2O)	0·497	0·482

*All properties reported on a mineral-matter-containing (mmc) basis.

Young's elastic modulus data are shown in Fig. 2. It is clear that there is a marked trend for E to increase with increasing bulk density. The values range from ~6 to 29 GN m^{-2} as the density increases from 0·70 to 0·99 Mg m^{-3}. These values compare favourably with those of ~2 to 5 GN m^{-2} reported by Bilimoria for low-density (0·65–0·80 Mg m^{-3}) formcoke specimens.[11] The values are relatively low compared to the value of 44 GN m^{-2} reported by Cost *et al.* for an isotropic polycrystalline graphite containing about 4% porosity.[12] This increase in Young's elastic modulus is related to the greater stiffness afforded by the higher solids content (lower porosity) of the denser specimens. This effect has been observed by many investigators; however, the exact relationship between elastic modulus and density or porosity has not been clearly defined. Several relationships have been proposed, but some fit well over only limited ranges of porosity, or violate the expected limiting values at zero or 100% porosity.

Mrozowski[13] found that a linear relation between Young's elastic modulus and porosity was the best fit for a low-porosity (<10%) graphite. A quadratic relation was proposed to describe the elastic modulus–porosity relationship by Spinner *et al.*[14] for materials with porosities as high as 30%. In addition to these linear and quadratic relations, several investigators have employed an exponential expression;[12,15–17] however, such an expression is frequently found to yield an increasing amount of error at higher porosities. It appears that one

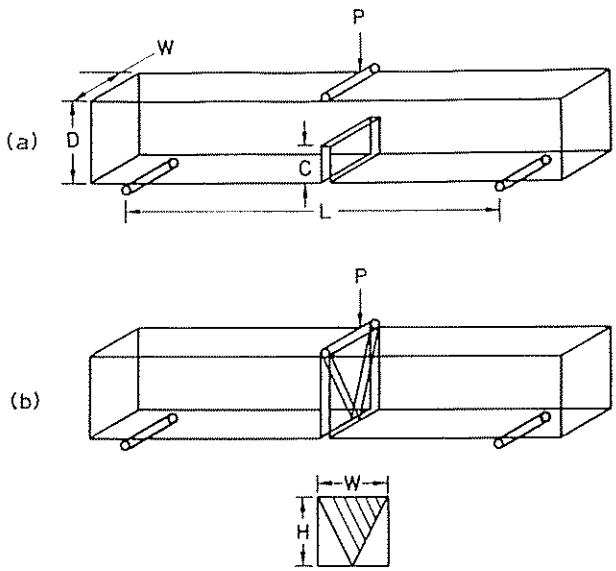

a notched-beam test; *b* work-of-fracture test

1 Specimen configurations

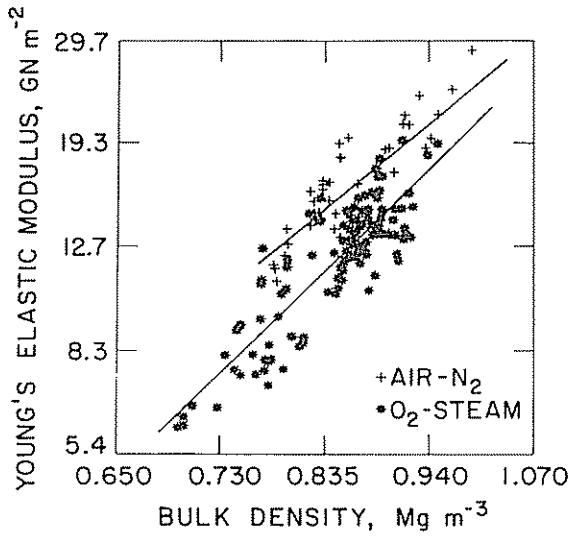

2 Young's elastic modulus as function of bulk density

solution may be to specify the range of porosities for which a given expression is known to be valid and to state the estimated amount of error to be expected.

In an effort to find a relation which best describes the data presented in Fig. 2, each of the expressions described above was implemented. None yielded a coefficient of determination (R^2) higher than 74%; a value of 100% indicates that all data fit the expression exactly. The amount of scatter in the data can only be partially attributed to the relatively poor fit of these models, since it is clear that parameters other than the bulk density must play a significant role in determining the elastic modulus. These include porosity, microcrack density, local char and binder distributions, ash content, and uniformity of carbonization from sample to sample. However, these parameters are either very highly correlated and would yield limited new information, or would require destruction of the specimen for their measurement, such that a prediction of Young's elastic modulus was not possible. It is therefore very difficult to improve upon these models simply by incorporating additional parameters.

Rather than retaining one of the three expressions presented above, a fourth type of relation was considered. It has the form:

$$E = E_0(\rho/\rho_0)^N \quad \ldots\ldots\ldots\ldots\ldots\ldots \quad (1)$$

where E_0 corresponds to the elastic modulus of a pore-free specimen, ρ_0 is the density of graphite (2·268 Mg m^{-3}), and E and ρ are the elastic modulus and density of a given formcoke specimen. The exponent N can be determined mathematically. The logarithmic transformation of this expression to linear form yields:

$$\ln E = \ln E_0 + N \ln(\rho/\rho_0) \quad \ldots\ldots\ldots\ldots\ldots\ldots \quad (2)$$

A linear regression of $\ln E$ on $\ln(\rho/\rho_0)$ gives an expression whose slope is the exponent N and whose y-intercept is $\ln E_0$. For the O_2–steam formcoke, this expression is:

$$\ln E = 1{\cdot}27 + 3{\cdot}32 \ln(\rho/\rho_0) \quad \ldots\ldots\ldots\ldots\ldots\ldots \quad (3)$$

This line is shown in Fig. 2 with the corresponding data. Similarly, for the air–N_2 formcoke the expression is:

$$\ln E = 12{\cdot}4 + 2{\cdot}79 \ln(\rho/\rho_0) \quad \ldots\ldots\ldots\ldots\ldots\ldots \quad (4)$$

This line is also shown in Fig. 2. All of the slope and intercept values, and coefficients of determination, are given in Table 4 for comparison. The t-ratios (parameter/standard deviation) and R^2 values indicate that the power-function model in equation (1) is the best fit for the formcoke data. Using the method described by Bowker and Lieberman,[18] the slopes and intercepts in equations (3) and (4) were tested to determine if the data for the two formcokes are statistically different. The test indicates that within 95% confidence two separate lines should be given as in Fig. 2, rather than only one line for the combined data.

According to the expressions described by equations (3) and (4), the value of the y-intercept is equal to $\ln E_0$. The values of E_0 calculated from the two regression equations are 330 and 240 GN m^{-2}, respectively. The average of the theoretical upper and lower limits on the elastic modulus of polycrystalline graphite was calculated according to the method described by Hill.[19] This value is known as E_{VRH} and is equal to 275 GN m^{-2}. The two values of E_0 determined for the formcokes are in good agreement with this theoretical value.

The data for the elastic shear modulus G are given in Fig. 3. These values are also presented as a function of the bulk density, and exhibit an increasing trend as was observed for Young's elastic modulus. The values range from ~3 to 10 GN m^{-2}. On fitting the data to the four different expressions discussed above, it was found that the power-function model again yielded the best fit. In the case of the elastic shear modulus, it has the form

$$G = G_0(\rho/\rho_0)^N \quad \ldots\ldots\ldots\ldots\ldots\ldots \quad (5)$$

The linearized form with the appropriate regression

Table 4 Comparison of mathematical models for Young's elastic modulus *v.* bulk density relationships

Model	Slope	Intercept	R^2	*t*-ratio Slope	*t*-ratio Intercept
Linear (E versus ρ)					
O_2–steam	44 031	−24 858	69	16·9	11·2
Air–N_2	56 240	−31 935	66	9·9	6·5
Combined	50 236	−29 210	57	10·6	15·5
Quadratic (E versus ρ^2)					
O_2–steam	266 362	−6747	68	1·68	5·8
Air–N_2	32 297	−7544	68	10·1	3·1
Combined	30 052	−830	58	15·7	5·9
Exponential ($\ln E$ versus ρ)					
O_2–steam	4·03	5·99	74	18·9	33·1
Air–N_2	3·21	6·93	67	9·9	24·8
Combined	4·01	6·06	63	17·3	30·7
Power [$\ln E$ versus $\ln(\rho/\rho_0)$]					
O_2–steam	3·32	12·68	74	19·3	74·4
Air–N_2	2·79	12·40	69	9·9	45·0
Combined	3·36	12·78	63	17·5	67·9

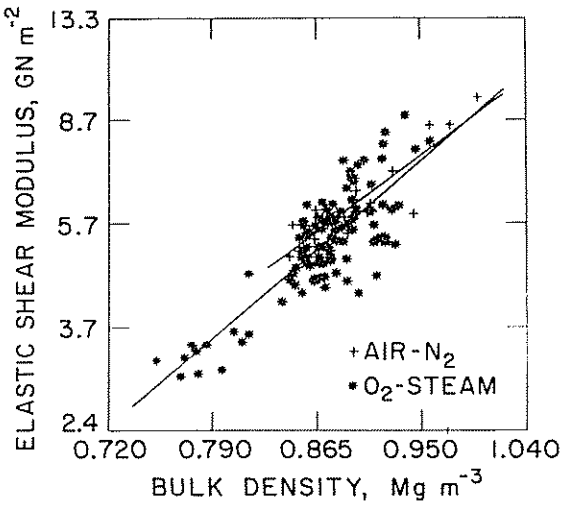

3 Elastic shear modulus as function of bulk density

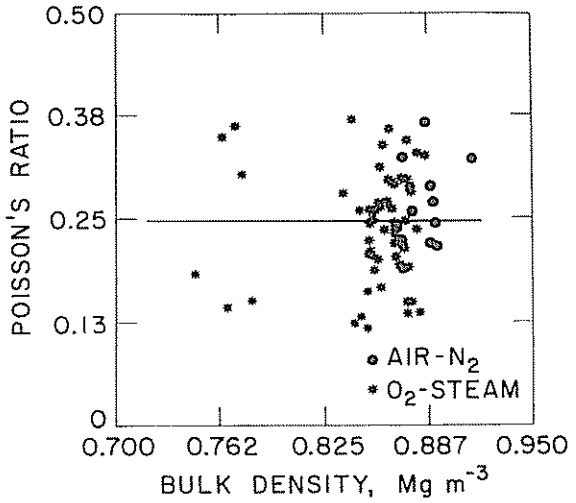

4 Poisson's ratio as function of bulk density

parameters for the O_2–steam formcoke is:

$$\ln G = 12{\cdot}30 + 3{\cdot}88\ln(\rho/\rho_0) \quad \ldots\ldots\ldots \quad (6)$$

and that for the air–N_2 formcoke is:

$$\ln G = 11{\cdot}89 + 3{\cdot}40\ln(\rho/\rho_0) \quad \ldots\ldots\ldots \quad (7)$$

As in the analysis of Young's elastic modulus, it was of interest to determine whether the data for the two formcokes could be combined or not. The same test method was again used to test for similarity of the two slopes and y-intercepts.[18] The test indicated that within 95% confidence either regression line was satisfactory to describe the data for both formcokes, and that the two data sets were statistically similar. As a result, both data sets were combined to obtain the single regression equation:

$$\ln G = 12{\cdot}32 + 3{\cdot}89\ln(\rho/\rho_0) \quad \ldots\ldots\ldots \quad (8)$$

which can be used to describe both sets of data. The logarithmic nature of the expression accounts for the fact that the regression parameters in equation (8) fall outside those of equations (6) and (7). It appears that the greater amount of scatter in the Young's modulus data, as compared with the shear-modulus data, results in the requirement of two separate regression lines for that parameter. There are no well defined microstructural differences in the two formcokes which can be assigned to this phenomenon.

Calculation of G_0 from the y-intercept of equation (8) yields a value of 220 GN m^{-2}, somewhat higher than the G_{VRH} value of 110 GN m^{-2}. The 95% confidence limits about the intercept extend to 140 GN m^{-2} at the lower limit, indicating that the difference between the two values is not very large.

The Poisson's ratio ν for each sample was calculated from its Young's modulus and shear modulus according to the expression:

$$\nu = \frac{E}{2G} - 1 \quad \ldots\ldots\ldots\ldots\ldots \quad (9)$$

The results are plotted versus bulk density in Fig. 4. The line on the plot is drawn through the average observed value of $\nu = 0{\cdot}25$. There was no statistical correlation of Poisson's ratio with bulk density. Examination of the relationship for Poisson's ratio given in equation (9) provides some insight into why no change was observed. The relative changes in E and G control the direction of change of Poisson's ratio. When E increases faster as a function of bulk density than G, the result is an increase in ν with bulk density. On the contrary, if E increases more slowly than G, a decrease in ν will be expected with increasing bulk density. In this study, the rates of change of E and G were very similar, resulting in no dependence of Poisson's ratio on the bulk density. A more detailed analysis of this functionality of Poisson's ratio has been presented by Gesing.[20]

FRACTURE TOUGHNESS

The fracture toughness K_{Ic} results for the formcokes are plotted as a function of the bulk density in Fig. 5. The data range from a minimum of 0·30 to a maximum of 0·75 MN m$^{-3/2}$. Another study on formcoke[11] reported fracture-toughness values of 0·16–0·36 MN m$^{-3/2}$ for bulk densities between 0·65 and 0·81 Mg m^{-3}. These data are in very good agreement as can be seen from Fig. 5. The values are higher than those of 0·03–0·05 Mg m$^{-3/2}$ reported by Advani *et al.*[21] for bituminous coals, as would be expected based on the more consistent structure obtained after carbonization of coal. However, the data are relatively low compared to the values of 0·5–1·5 MN m$^{-3/2}$ which have been reported for graphite.[22,23] This can also be explained in terms of the relatively low Young's elastic moduli observed for the formcokes, a parameter directly related to the fracture toughness according to:

$$K_{Ic} = (2E\gamma_f)^{1/2} \quad \ldots\ldots\ldots\ldots\ldots \quad (10)$$

where γ_f is the fracture initiation surface energy, which is discussed below.

As with the elastic moduli, the fracture toughness also

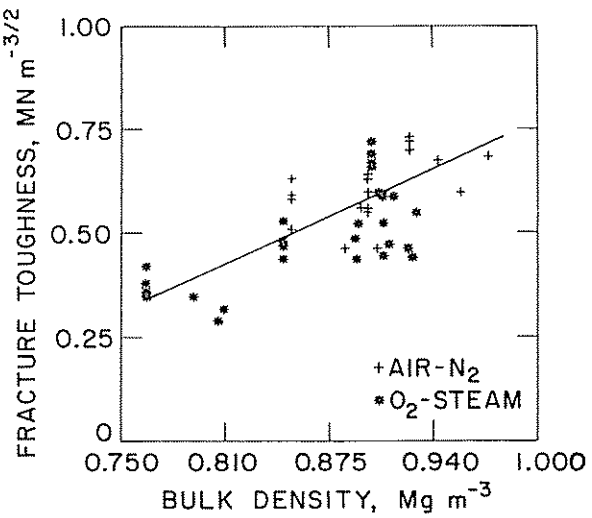

5 Fracture toughness as function of bulk density

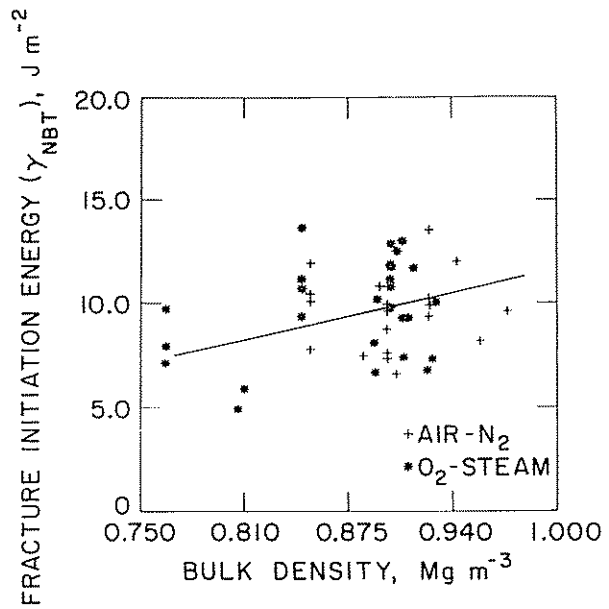

6 Fracture initiation surface energy as function of bulk density

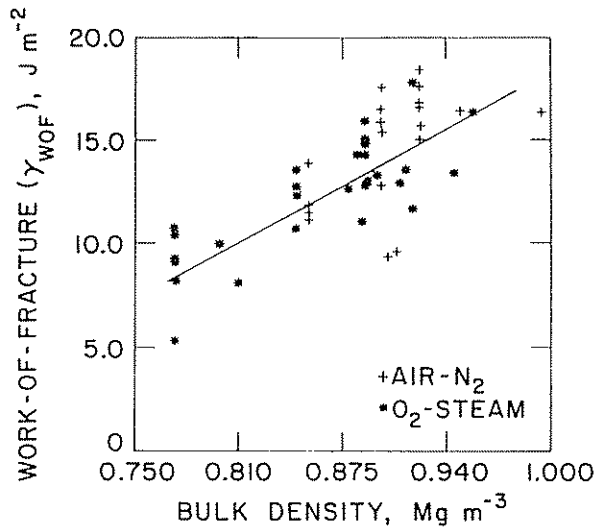

7 Fracture propagation surface energy as function of bulk density

increases with increasing bulk density. Because of the destructive nature of the notched-beam test, fewer data points were collected for this parameter. Consequently, the data for both formcokes were combined and a simple linear regression analysis was completed. No improvement in the fit of the data was observed with the other three expressions described above. The linear regression line is included in Fig. 5 and is given by:

$$K_{1c} = -1{\cdot}06 + 1{\cdot}83\rho \quad \ldots\ldots\ldots\ldots (11)$$

It may be noted that this expression differs from those for the elastic moduli not only in that it is a simple linear expression, but also because the fracture toughness and density of polycrystalline graphite are not used as normalizing parameters in this case. Such a treatment is difficult to apply to the fracture toughness for it may be possible for specimens of less than theoretical density to have a higher fracture toughness than that of theoretically dense graphite, a hypothetical value which in itself is not known reliably. For certain cases microcracks, porosity, and foreign inclusions which would lower the density have been demonstrated to be involved in the dissipation of energy in the crack tip process zone, such that an effectively higher stress is required to fracture the specimen.[24] Since the fracture toughness is directly related to the fracture stress, an apparently higher value is measured. It is because of these potential complications in the relationship of the fracture toughness to the bulk density that the simple linear model was retained. The increasing trend of the fracture toughness with increasing bulk density indicates that for specimens containing similar flaw sizes, the denser specimens will be stronger and sustain a higher applied stress before fracture occurs.

FRACTURE SURFACE ENERGY

Two types of fracture surface energy were measured for the formcoke specimens, the fracture initiation energy γ_{NBT} and the fracture propagation energy γ_{WOF}. The first of these is presented as a plot of the surface energy for fracture initiation *v.* the bulk density in Fig. 6. The fracture initiation energy is calculated from two experimentally determined parameters, the fracture toughness and the Young's elastic modulus of the specimen, according to equation (10). For this reason, the amount of scatter in the data is compounded, but a trend for γ_{NBT} to increase with the bulk density is observed. The lowest values, ~5 J m^{-2}, were observed for the O_2–steam formcoke. The highest values observed were about 13 J m^{-2} for the higher-density air–N_2 formcoke specimens. The observed fracture initiation energies for the formcokes are relatively low compared with those for polycrystalline graphites, which range from 20 to 80 J m^{-2} as reported in the literature.[22,23] The weaker bonding and lower density of the formcokes allow for their easier fracture initiation, and therefore lower fracture initiation energies are measured.

The least-squares regression line for the combined data of the two formcokes is shown on Fig. 6 and has the form:

$$\gamma_{NBT} = -6{\cdot}43 + 18{\cdot}1\rho \quad \ldots\ldots\ldots\ldots (12)$$

The increase in γ_{NBT} with increasing bulk density can be simply explained in terms of the fracture surface area. Specimens with a lower bulk density contain less mass per unit volume and correspondingly fewer bonds or a smaller amount of material through which the crack must travel. Less energy, therefore, is required to initiate crack extension for the lower-density specimens.

The work of fracture or fracture propagation surface energy is a measure of the energy required to propagate stably a crack through the formcoke. It is presented as a function of the bulk density in Fig. 7. As for all the other mechanical properties investigated, the work of fracture also exhibits significant correlation with the bulk density. A trend for the work of fracture γ_{WOF} to increase with the bulk density exists. The values of the crack propagation energy range from ~6 to 18 J m^{-2}. These energies are significantly less than the work-of-fracture values of 100–150 J m^{-2} reported in the literature for bulk polycrystalline graphites.[25,26] The high porosity and the less dense structure of the formcokes apparently result in a much easier fracture path, and therefore a smaller consumption of energy during crack propagation than is reported for the graphites. The least-squares regression line is shown for the combined data of the two formcokes because of the limited data available when they are considered separately. It has the form:

$$\gamma_{WOF} = -23{\cdot}7 + 41{\cdot}9\rho \quad \ldots\ldots\ldots\ldots (13)$$

The lower values of γ_{WOF} for the lower bulk densities are, of course, related to the smaller fracture surface area traversed by the crack as described above.

The closeness or similarity of the energies required for fracture initiation and fracture propagation is also of interest. The small difference indicates little resistance to

crack propagation once fracture has been initiated. In contrast, fracture energies reported for polycrystalline graphite indicate a much larger difference between the energy for crack initiation and the energy for crack propagation and, therefore, greater resistance to crack growth. The regression parameters obtained for these two energies reveal that the fracture propagation energy increases faster with bulk density than the fracture initiation energy, since the slope of the former equation is greater. This trend would be of greater consequence at low densities such as those resulting after partial gasification of specimens. In such a case, the energy to initiate fracture would be less but would be essentially sufficient to result in fracture propagation entirely through the material.

SUMMARY AND CONCLUSIONS

An extensive statistical analysis of the Young's elastic modulus data as a function of bulk density resulted in the selection of a power-function relationship as the one best describing the data. It has the form $E = E_0(\rho/\rho_0)^N$. An analogous expression was found to describe the elastic shear modulus data best. Calculation of the values of E_0 and G_0 from the regression parameters yielded values very close to the expected E_{VRH} average values for theoretically dense polycrystalline graphite, adding further credibility to the model. The lack of correlation of Poisson's ratio with bulk density indicates that rates of change of Young's elastic modulus and the elastic shear modulus with bulk density are very similar. The fracture toughness and fracture surface energies exhibited increasing trends with increasing bulk density similar to the elastic moduli. The values for the fracture initiation and fracture propagation surface energies were very similar. Their proximity indicates that little resistance to crack propagation is offered once fracture has been initiated. It also suggests poor thermal shock resistance.

Overall, the brittle-materials mechanical-properties tests used in this study of formcoke were found to be useful in characterizing the materials. It would be favourable to increase the values of the properties investigated in this study in order to improve the mechanical integrity of the formcoke. This would require an increase in bulk density and a decrease in porosity, which would have certain implications with respect to formcoke reactivity. An acceptable compromise to obtain the desired formcoke characteristics would therefore have to be selected. The data reported here would be valuable in making comparisons with future similar measurements of coke mechanical properties from the wide variety of possible fabrication methods.

ACKNOWLEDGMENTS

This research was supported by a fellowship for Dr Easler from Inland Steel Co. The authors appreciate having helpful discussions with Drs W. DuBroff and E. Spearin of Inland Steel Co. concerning this research.

REFERENCES

1. J. E. BARKER: *J. Iron Steel Inst.*, 1971, **209**, 100–108.
2. J. K. HOLGATE and P. H. PINCHBECK: *J. Iron Steel Inst.*, 1973, **211**, 547–566.
3. J. WORK: *J. Met.*, 1966, **18**, (5), 635–642.
4. R. F. MORAN and R. T. JOSEPH: *Trans. AIME Soc. Min. Eng.*, 1976, **260**, (3), 29–32.
5. M. HIGUCHI *et al.*: in 'Coal, coke, and the blast furnace', 19–28; 1978, London, The Metals Society.
6. S. SPINNER and W. E. TEFT: *Proc. ASTM*, 1961, **61**, 1221–1238.
7. W. R. DAVIS: *Trans. Br. Ceram. Soc.*, 1968, **67**, 515–541.
8. A. G. EVANS: in 'Fracture mechanics of ceramics', Vol. 1, 17–48; 1973, New York, Plenum Press.
9. R. W. DAVIDGE and G. TAPPIN: *J. Mater. Sci.*, 1968, **3**, 164–173.
10. D. A. SUMMERS, J. CORWINE, and LI-KING CHEN: in 'Proc. of 12th symp. on rock mechanics', 241–261; 1970, University of Missouri at Rolla, University of Missouri–Rolla Press.
11. Y. F. BILIMORIA: PhD thesis, Illinois Institute of Technology, 1982.
12. J. R. COST, K. R. JANOWSKI, and R. C. ROSSI: *Philos. Mag.*, 1968, **17**, (148), 851–854.
13. S. MROZOWSKI: in 'Proc. of 1st and 2nd conf. on carbon', 31; 1954, Baltimore, Waverly Press.
14. S. SPINNER, F. P. KNUDSEN, and L. STONE: *J. Res. Natl Bur. Stand., Eng. Instrum.*, 1963, **67C**, (1), 39–46.
15. R. M. SPRIGGS and L. A. BRISSETTE: *J. Am. Ceram. Soc.*, 1962, **45**, (4), 198–199.
16. R. M. SPRIGGS, L. A. BRISSETTE, and T. VASILOS: *J. Am. Ceram. Soc.*, 1962, **45**, (8), 400.
17. F. P. KNUDSEN: *J. Am. Ceram. Soc.*, 1962, **45**, (2), 94–95.
18. A. H. BOWKER and G. J. LIEBERMAN: 'Engineering statistics'; 1959, New Jersey, Prentice-Hall.
19. R. HILL: *Proc. Phys. Soc. (Lond.)*, 1952, **65A**, (5), 349–354.
20. A. J. GESING: PhD thesis, Pennsylvania State University, 1982.
21. S. H. ADVANI, Y. T. LIN, F. D. GMEINDL, and W. R. POWELL: in 'Proc. 4th underground coal conversion symp.', 507–514; 1978, Report SAND-78-0941, Sandia National Laboratory, Albuquerque, N. Mex.
22. J. L. WOOD, R. C. BRADT, and P. L. WALKER, Jr: *Carbon*, 1980, **18**, (3), 169–178.
23. G. T. YAHR, R. S. VALACHOVIC, and W. L. GREENSTREET: in 'Proc. 10th biennial conf. on carbon', 223–225; 1971, Lehigh University, Pa, Lehigh University Press.
24. F. E. BURESCH: in 'Fracture mechanics of ceramics', Vol. 4, 835–847; 1978, New York, Plenum Press.
25. A. G. TATTERSALL and G. TAPPIN: *J. Mater. Sci.*, 1966, **1**, (3), 296–301.
26. F. CLARKE, H. G. TATTERSALL, and G. TAPPIN: *Proc. Br. Ceram. Soc.*, 1966, (6), 163–172.

Research on metallurgical slags at Glasgow and its contribution to refractories research

R. I. Robertson, P. L. Smith, and J. White

The emergence in Glasgow in the 1930s of a research school in chemical metallurgy, concerned largely with slag chemistry, and its extension into the field of refractories research are described. Particular interests at that time included phase relationships governing the mineralogical constitution and melting–composition relationships in slags and refractories and redox equilibrium in slag- and refractory-forming systems. Ways in which these approaches, and their extension into the area of applied thermodynamics, have contributed to refractories research are indicated with illustrations from the fields of both oxide- and non-oxide refractories. IS/599

 This paper was presented at the conference to mark the centenary of teaching of Metallurgy in Glasgow held in the Department of Metallurgy, University of Strathclyde, Glasgow, on 25–26 June 1984, and is published here by courtesy of the University of Strathclyde. Dr Robertson and Dr Smith are with GR-Stein Refractories Ltd, Sheffield. Professor White, who was formerly Head of the Department of Ceramics, is an Emeritus Professor of the University of Sheffield.

EARLY SLAG RESEARCH AT GLASGOW

Although the phase diagrams of a number of oxide and oxide–sulphide combinations occurring in inclusions in steel had been studied earlier at Glasgow under Professor Andrew, it was in the 1930s, under Professor Hay, that a programme of research on slag-forming oxide systems took shape. In the present paper research in the refractories field is described which can be considered to have stemmed from this earlier Glasgow work on metallurgical slags.

At that time, the concept of the slag as a medium having interfaces with three other media, the liquid metal, the furnace atmosphere, and the refractory lining of the furnace, and tending continuously towards three different equilibrium states across these interfaces, had already emerged. It was also recognized that to perform their refining function, slags should be reasonably fluid (implying restrictions both on intrinsic viscosity and on the quantity of solid phases that could be carried in suspension) and that their chemistry should be such that the oxidized 'metalloids' entering the slag from the metal should be stabilized in the oxidized state to enable refining to proceed.

In its initial stages, the Glasgow programme was concerned primarily with the study of phase equilibrium in simple binary and ternary systems, which, it was hoped, would enable the temperature and composition limits of the liquid phase in actual slags to be defined. The method used to determine the temperatures of phase changes was the metallurgist's technique of heating and cooling curves, which was not particularly well suited to the study of oxide systems even though considerable ingenuity was expended in increasing its accuracy and sensitivity. In addition, a thermobalance capable of operating to over 1700°C at controlled oxygen pressure was constructed to study the gas phase determined redox (Fe^{3+}–Fe^{2+}) equilibrium in oxide melts, which was considered to be an important variable determining oxygen transfer to the metal by actual slags.

No direct studies of slag–metal or refractory–metal equilibria were attempted at that time, however, although both aspects were to receive attention from later workers at Glasgow, including of course Professor Bell. Instead the growing interest in refractories, particularly basic refractories, which were then undergoing rapid development, led to an increasing interest in refractory applications of the work.

SOLID-PHASE COMPATIBILITIES IN BASIC SLAGS AND REFRACTORIES

The classical demonstration of the value of phase-diagram research in the refractories field is still that provided by the development of the superduty silica brick in the early 1940s.[1,2] This development was based on the earlier findings[3] that, in the systems CaO–SiO_2, MgO–SiO_2, and FeO–SiO_2, compositions rich in SiO_2 form two immiscible liquids on melting, whereas in the system Al_2O_3–SiO_2 no liquid immiscibility occurs. Hence the presence of quite small amounts of Al_2O_3 (as little as 0·8%) in silica refractories increases the solubility of the SiO_2 in the liquid phase formed at high temperatures quite dramatically, lowering their temperature of subsidence under load and decreasing their resistance to slags containing CaO or FeO.

The attainment of a similar understanding of the relation between composition and performance of basic refractories has proved more difficult to achieve because of the number of significant components involved.

In Glasgow the first step towards a solution of this problem was taken when the device was adopted of constructing tables to show the assemblages (combinations) of mutually compatible phases which would occur within the composition range of interest in basic slags.[4] These assemblages were arrived at by a process which involved writing down, for each phase, all the other phases capable of coexisting with it as indicated by known binary, ternary, etc., phase diagrams, arranging these in groups having the selected phase in common and then eliminating those phases which, although they could exist singly with the selected phase, were shown by known phase diagrams to be mutually incompatible with each other.

The first scheme of phase assemblages proposed for phosphate-containing basic slags contained a systematic error due to an error in a published phase diagram but this was later corrected.[5] Subsequently, a modified version of the corrected scheme was constructed to cover the phase assemblages containing periclase in the system CaO–MgO–FeO–Fe_2O_3–Al_2O_3–Cr_2O_3–SiO_2, to which phosphate-free basic refractories could be considered to belong.[6–8]

Table 1 presents an updated version of this scheme. Points to note are that the silicates coexisting with periclase (magnesiowüstite) are those which coexist with it